Talanta 83 (2011) 1335–1340

Contents lists available at ScienceDirect

Talanta

journal homepage: www.elsevier.com/locate/talanta

CdSe quantum dots capped PAMAM dendrimer nanocomposites for sensing nitroaromatic compounds

M. Algarra[a], B.B. Campos[b], M.S. Miranda[a], Joaquim C.G. Esteves da Silva[b,*]

[a] Centro de Geologia da Universidade do Porto, Departamento de Geociências, Ambiente e Ordenamento do Território do Porto, Faculdade de Ciências da Universidade do Porto, Porto, Portugal
[b] Centro de Investigação em Química, Departamento de Química e Bioquímica, Faculdade de Ciências da Universidade do Porto, Porto, Portugal

ARTICLE INFO

Article history:
Received 20 September 2010
Received in revised form 20 October 2010
Accepted 29 October 2010
Available online 13 November 2010

Keywords:
CdSe quantum dots
PAMAM-G_4 dendrimer
Nanocomposites
Explosives
Nitroaromatic compounds

ABSTRACT

The detection of nitroaromatic compounds, best known as raw materials in explosives preparations, is important in many fields including environmental science, public security and forensics. CdSe quantum dots capped with PAMAM-G_4 dendrimer were synthetized in water and used for the detection of trace amounts of three nitroaromatic compounds: 4-methoxy-2-nitrophenol (MNP), 2-amine-5-chloro-1,3-dinitrobenzene (ACNB) and 3-methoxy-4-nitrobenzoic acid (MNB). To increase the apparent water solubility of these compounds α-cyclodextrin (α-CD) was used to promote the formation of inclusion complexes. The studied nitroaromatic compounds (plus α-CD) significantly quenched the fluorescence intensity of the nanocomposite with linear Stern–Volmer plots. The Stern–Volmer constants (standard deviation in parenthesis) were: MNB, $K_{SV} = 65(5) \times 10^4\ M^{-1}$; ACNB, $K_{SV} = 19(2) \times 10^4\ M^{-1}$; and, MNP, $K_{SV} = 33(1) \times 10^2\ M^{-1}$. These constants suggest the formation of a ground state complex between the nitroaromatric compounds and the sensor which confers a relatively high analytical sensitivity. The detection sensibilities are about 0.01 mg L^{-1} for MNB and ACNB and about 0.1 mg L^{-1} for MNP. No interferences or small interferences are observed for trinitrotoluene [$K_{SV} = 10(2) \times 10^2 \times M^{-1}$], 2,4-dinitrotoluene [$K_{SV} = 20(3) \times 10\ M^{-1}$], 2,6-dinitrotoluene [$K_{SV} = 11(4) \times 10\ M^{-1}$] and nitrobenzene [$K_{SV} = 2(1) \times 10^3 \times M^{-1}$].

1. Introduction

Nitroaromatic compounds are produced in large scale in the chemical industry. They are used in the manufacture of pesticides, dyes, pharmaceuticals and are raw materials in explosives preparations [1].

The detection of trace amounts of nitroaromatic compounds is an important task in many fields including environmental science, public security and forensic science. In environmental science, nitroaromatic compounds have received a great deal of attention over the years because these compounds present a high toxicity and have been proved to be potential carcinogens or mutagens which are dispersed to soils, water and air as consequence of their utilization [2]. Moreover, they are known to undergo microbiological and photochemical degradation processes in the environment leading to the formation of other nitroaromatic compounds. In public security, there is concern about unexploded land mines and to the increasing incidents and threats of terrorist attacks with explosive devices. In forensics, the detection of trace amounts of nitroaromatic explosives in the body or clothes may lead to the identification of persons in recent contact with explosives.

Many expensive and operator dependent analytical methodologies exist to detect nitroaromatic explosives: mass spectrometry [3–5]; surface enhanced Raman spectroscopy [6]; nuclear quadrupole resonance [7–9]; energy dispersive [10]; X-ray diffraction [11–13]; neutron activation analysis [14,15]; ion mobility spectrometry [16]; and, electrochemistry [17,20]. Fluorescence and luminescence based techniques for the detection of nitroaromatic compounds offer many benefits over other commonly used methodologies, although nitroaromalic compounds are not intrinsically fluorescent. Many nitroalkane explosives, such as nitroamines, nitrate esters, and peroxide explosives have non conjugated structures that allow efficient vibrational relaxation. Nitroaromatic explosives, despite having an aromatic structure, do not fluoresce as result of the strong electron-withdrawing nature of the nitro substituents. In spite of this lack of native fluorescence, many methods have been proposed in recent years for their detection using luminescence based techniques. In this respect fluorescence based sensors are very promising [21–25].

Nanotechnology designed new materials can be used for trace detection of nitroaromatic compounds [26]. Semiconduc-

---

* Corresponding author. Tel.: +351 220 402 569; fax: +351 220 402 654.
E-mail address: jcsilva@fc.up.pt (J.C.G.E. da Silva).

0039-9140/$ – see front matter © 2010 Elsevier B.V. All rights reserved.
doi:10.1016/j.talanta.2010.10.056

tor nanocrystals, such as CdS, CdSe or CdTe, known as quantum dots (QDs) show high photoluminescence efficiency, robustness and flexibility of functionalization with conjugating ligands for the selective nanosensing of analytes [27–35]. The applications of QDs in the detection of nitroaromatic compounds, based on direct fluorescence quenching of QDs [36,37] or fluorescence resonance energy transfer [38], have been proposed. The detection of a nitroalkane explosive, nitromethane, based on the quenching of the fluorescence intensity of a hybrid cadmium sulfide QDs dendrimer DAB-G_5 nanocomposite has been studied [39]. Besides the capping agent of QDs using simple thiolate reagents that confers to them water solubility, stability and chemical reactivity, dendrimers are being used as coating polymers of QDs. The conjugation of dendrimers with QDs, originating hybrid nanomaterials, markedly increases their physico-chemical properties rendering them biocompatibility and biostability, increased reactivity, and confers an important biomedical role in diagnostics and biochemical sensing [40–42].

This paper reports the synthesis of a hybrid CdSe QDs dendrimer PAMAM generation 4 in water–CdSe–PAMAM-G_4 nanocomposites. The quenching of the fluorescence of CdSe-PAMAM nanocomposites by three nitroaromatic compounds 4-methoxy-2-nitrophenol (MNP), 3-methoxy-4-nitrobenzoic acid (MNB) and 2-amine-5-chloro-1,3-dinitrobenzene (ACNB) is presented and its potential application for sensing of these materials assessed. Nitrophenols nitrobenzoic acids and nitroanilines are known to be intermediates in the environmental degradation of nitroaromatic explosives [43]. Also, the effect of trinitrotoluene (TNT), 2,4-dinitrotoluene (2,4-DNT), 2,6-dinitrotoluene (2,6-DNT) and nitrobenzene (NB) in the fluorescence of the nanocomposite was evaluated.

The nanocomposites synthetic procedure used in this work uses a green chemistry approach because it was based on water instead of using organic solvents [44,45]. The selection of the PAMAM-G_4 dendrimer was based on previous studies where it was demonstrated that the interaction with CdSe nanocrystals increased with the generation of the dendrimer [45].

2. Materials and methods

2.1. Reagents and apparatus

Polyamidoamine dendrimer-1,12-diaminododecane core-generation 4 (PAMAM-G_4, solution in methanol 10%), cadmium chloride (99.9%, $CdCl_2$), selenium powder (Se, 99.99%), α-cyclodextrin, and nitroaromatic compounds: 4-methoxy-2-nitrophenol (MNP); 2-amine-5-chloro-1,3-dinitrobenzene (ACNB); 3-methoxy-4-nitrobenzoic acid (MNB); trinitrotoluene (TNT); 2,4-dinitrotoluene (2,4-DNT); 2,6-dinitrotoluene (2,6-DNT); and, nitrobenzene (NB) were purchased from Sigma–Aldrich Spain; sodium borohydride ($NaBH_4$, ≥96%) and 3-mercaptopropinoic acid (MPA, 99%) were purchased from Fluka and used without further purification. Stock solutions ($50\,mg\,L^{-1}$) of MNP, ACNB and MNB were prepared by rigorous weighting of the powders in aqueous solutions of α-CD (10^{-2} M). Concentrated stock solutions ($1000\,mg\,L^{-1}$) of TNT, 2,4-DNT, 2,6-DNT and NB were prepared in acetonitrile and diluted stock solutions ($50\,mg\,L^{-1}$) in aqueous solutions of α-CD (10^{-2} M) were obtained by rigorous dilution of the concentrated solution.

Photoluminescence measurements were recorded with a Horiba Jovin Yvon Fluoromax 4 TCSPC spectrophotometer using an excitation of 380 nm and an emission range of 400–740 nm, with an integration time of 0.1 s and a slit of 5 nm. Samples were contained in 1-cm path length quartz cuvettes. The Quantum yield (QY) was determined using Rhodamine 6G as a standard. Rhodamine 6G has a QY of 90% at an excitation wavelength of 488 nm in methanol [18]. The calibration curve for Rhodamine was obtained in methanol which has a refractive index (n_{st}) of 1.329. The integrated area under the fluorescence curves (excitation at 488 nm) was plotted versus the absorbance at 488 nm (after subtraction of the solvent absorbance) for different concentrations. The same procedure was repeated for the QD samples dissolved in deionized water ($n = 1.3749$). The excitation intensity and slit width were held constant for all measurements. The QY of the QDs was obtained from:

$$\mathrm{QY}_{\mathrm{QD}} = \mathrm{QY}_{\mathrm{st}} \left[\frac{(dI/dA)_{\mathrm{QD}}}{(dI/dA)_{\mathrm{st}}}\right] \left[\frac{n^2_{\mathrm{QD}}}{n^2_{\mathrm{st}}}\right]$$

where I is the area under the PL curves and A is the corresponding absorbance [19]

Scanning electron microscopy (SEM) and Energy dispersive X-Ray analysis (EDS) were recorded by means of a FEI Quanta 400FEG/EDAX Genesis X4M high resolution scanning electronic microscope to examine the morphology of the nanocomposites obtained.

2.2. Preparation of CdSe-PAMAM nanocomposites

CdSe-PAMAM nanocomposites were prepared in three major steps:

(i) Selenium was reduced according to the following chemical reaction:

$$4NaBH_4(aq) + 2Se(s) + 7H_2O(l) \rightarrow 2NaHSe(aq) + Na_2B_4O_7(s) + 14H_2(g)$$

60 mg of $NaBH_4$ and 50 mg of Se were dissolved in 3 mL of deionized water and left 12 h under nitrogen atmosphere. The obtained solution goes from colorless to brown-red.

(ii) 90 μL of PAMAM-G_4 (6.31×10^{-4} mmol) were mixed with 25 mL of water and the mixture was stirred until the dissolution was completed. Then, 10 mg of $CdCl_2$ (0.05 mmol) was added and left to stabilize for 3 h followed by addition of 100 μL (1.14 mmol) of MPA. According to previous experiments, this concentration for MPA is the best ratio to PAMAM (MPA:PAMAM 230:1) because as the concentration of MPA increases the pH of the aqueous solution decreases.

(iii) After 24 h, 100 μL of the reduced selenium solution (i), was added to solution (ii), with continuously stirring for more 24 h, yielding a orange-red solution that was dialyzed in cellophane membrane (using a MW CO 12,000–14,000 Dalton dialysis tube from Medicell International) for 12 h against deionised water at room temperature. The CdSe-PAMAM solution was centrifuged at 13,000 rpm for 10 min to remove unreacted reactants.

2.3. Quenching of CdSe-PAMAM nanocomposites by nitroaromatic compounds

For photoluminescent measurements CdSe-PAMAM (500 μL) was transferred to a 5 mL calibrated flask together with aliquots containing from 4.60×10^{-5} to 2.3×10^{-1} M of nitroaromatic compounds and fulfilled with α-CD (10^{-2} M) – the problem of small solubility of these compounds in aqueous solution was solved by using the inclusion complex with α-CD [20]. The samples were sonicated for 30 min, left until room temperature was reached, and then the fluorescence spectra were recorded.

2.4. Data analysis

A preliminary screening analysis was performed following a Placket–Burman design, focusing on the effect's evaluation of the concentrations of the nitroaromatic compounds (MNP, ACNB, MNB) and α-CD. The experimental design formulation and the corresponding analysis of the effects (ANOVA) and response surface calculations were done using the Unscramble v 9.2 (CAMO PROCESS AS, Oslo, Norway).

In this study quenching of fluorescence by nitroaromatic compounds was described using the Stern–Volmer equation [44]:

$$\frac{I_0}{I} = 1 + K_{sv}[\text{Nitroaromatic}]$$

where I_0 is the fluorescence intensity without nitroaromatic compounds, I is the fluorescence intensity observed in the presence of the nitroaromatic compounds and K_{SV} is the Stern–Volmer constant.

3. Results and discussion

3.1. Characterization of the CdSe-PAMAM nanocomposite

Fig. 1a shows the EDS spectra of the purified CdSe-PAMAM nanocomposites. The presence of the signals due to elements Cd and Se shows the composition of the QDs, the presence of the elements C and N confirms that the synthesized material is indeed PAMAM capped to CdSe QDs, the detection of the elements O, C and the strongest signal of S suggests that MPA is bound to the CdSe QDs. SEM images of the purified CdSe-PAMAM nanocomposites (Fig. 1b and c) do not give information about the morphology of the material but amorphous microscopic spherical structures of sizes between 25 and 100 nm can be observed. The comparison of the SEM images of CdSe-PAMAM-G_4 nanocomposites recorded with the secondary electron (Fig. 1b) and the back-scattered (Fig. 1c) electron detector shows that the QDs are homogenously distributed throughout the nanocomposite. CdSe-PAMAM solutions, kept at room temperature and protected from light, were stable in aqueous solution without noticeable precipitation and their spectroscopic behavior do not show marked variation for at least three months.

The photoluminescent emission spectrum of CdSe-PAMAM in aqueous solution (excitation at 380 nm) is characterized by a broad band in the 400–750 nm range with a maximum at 570 nm (Stokes shift of 190 nm) – it shows a strong orange emission.

The luminescence properties of dendrimer QDs nanocomposites are somewhat dependent of the synthesis process [39]. In this study it was monitorized the effect of the stirring process in the maximum wavelength of the CdSe-PAMAM nanocomposite and it was observed that after 24 h the maximum intensity of the emission spectrum is constant at 570 nm. The quantum yield (QY) of CdSe-PAMAM nanocomposite has a value of 1.8%, which is a relatively low value for QDs. This small QY is due to the fact that the material has a major non-fluorescent component, the dendrimer, that limits its fluorescence efficiency.

3.2. Screening analysis of the factors affecting the fluorescence

The development of an aqueous based sensor for nitroaromatic compounds has a critical limitation due to the small water solubility of some of these substances. To deal with this characteristic of nitroaromatic compounds, the increase of the apparent solubility as consequence of the formation of an inclusion complex with α-cyclodextrin was analysed.

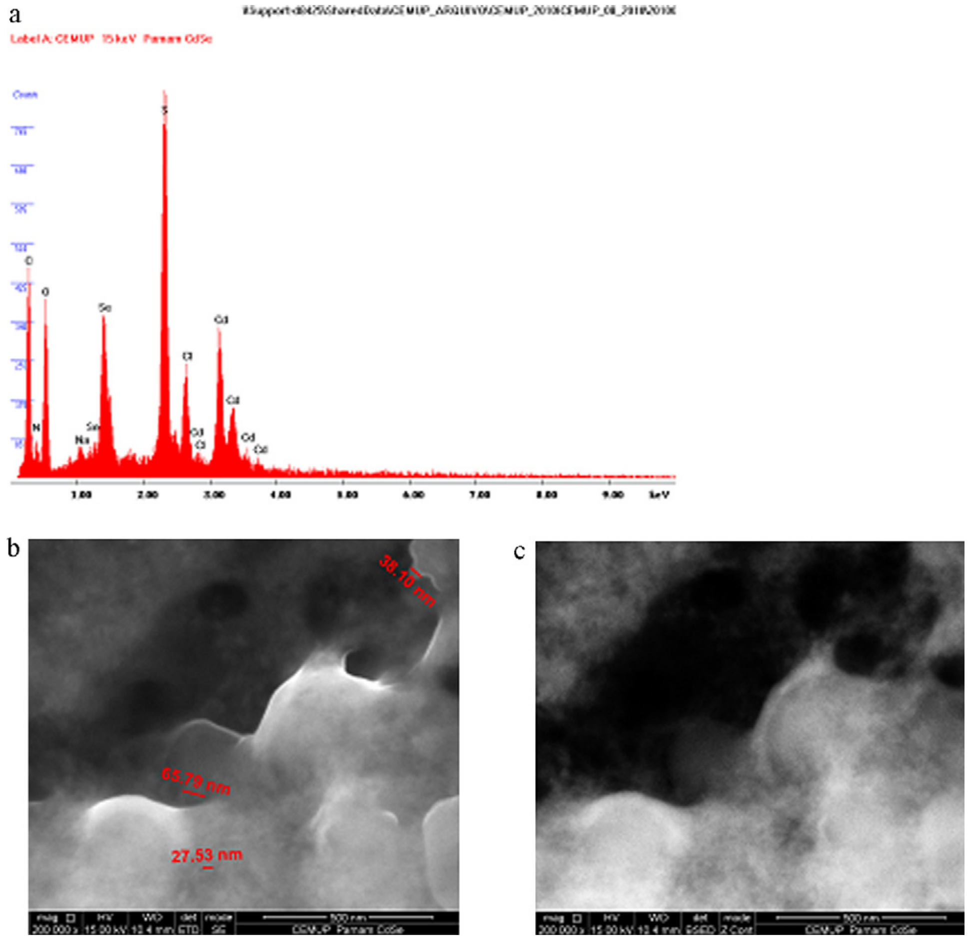

Fig. 1. EDS (a.) and SEM images of CdSe-PAMAM-G_4 nanocomposite recorded with the secondary electron (b.) and the back-scattered (c.) electron detector.

Table 1
Levels of the substances used in the Plackett–Burman screening design.

Substance	Level −1	Level +1
MNP (ppm)	0.1	0.5
ACNB (ppm)	0.01	0.1
MNB (ppm)	0.01	0.1
Nanocomposite (mL)	0.5	1
α-CD (M)	1×10^{-4}	1×10^{-3}

In order to investigate the effect of the five substances (the three nitroaromatic compounds, the nanocomposite PAMAM-CdSe QDs and α-CD) on the fluorescence of the nanocomposite an experimental design, based on a Placket–Burman design of five factors and two levels (8 experiments), was used [47–50]. Table 1 shows the factors and levels used and Table 2 shows the corresponding ANOVA table.

The analysis of Table 2 shows the following:

(i) As expected, the concentration of the nanocomposite (the fluorophore) has the highest significance with a *F*-ratio 1.43×10^3. This result confirms that increasing the concentration of the PAMAM-CdSe QDs the fluorescence also increases.

(ii) The other analysed substances, with the exception of ACNB which provokes no significative fluorescence variation, have a relatively small effect on the fluorescence. Indeed, although the corresponding *F*-ratios are relatively small the *b*-coefficients are higher than the corresponding errors [47–50].

As suggested the effect of α-CD is to provoke an increase of the fluorescence probably due to an increase of water solubility of the nitroaromatic compounds. Due to this result, the effect of the nitroaromatic compounds will be assessed in the presence of α-CD.

3.3. Effect of nitroaromatic compounds on the fluorescence spectra of the PAMAM-CdSe nanocomposites

Fig. 2 shows the effect of the nitroaromatic compounds MNP, ACNB and MNB, in the presence of α-CD, on the fluorescence of the PAMAM-CdSe nanocomposites. This figure shows that these substances provoke a marked quenching of the fluorescence. In order to quantify the quenching, Stern–Volmer plots were done and the results are presented in Table 3.

Linear Stern–Volmer plots were obtained that shows different sensibilities for the three nitroaromatic compounds plus α-CD: MNB provokes the highest quenching [$K_{SV} = 65(5) \times 10^4\ \mathrm{M^{-1}}$], followed by ACNB [$K_{SV} = 19(2) \times 10^4\ \mathrm{M^{-1}}$] and MNP provokes a relatively small quenching [$K_{SV} = 33(1) \times 10^2\ \mathrm{M^{-1}}$]. These results suggest that concentrations higher than 0.01 mg L^{-1} of MNB and ACNB and higher than 0.1 mg L^{-1} of MNP provoke measurable quenching on the nanocomposite fluorescence.

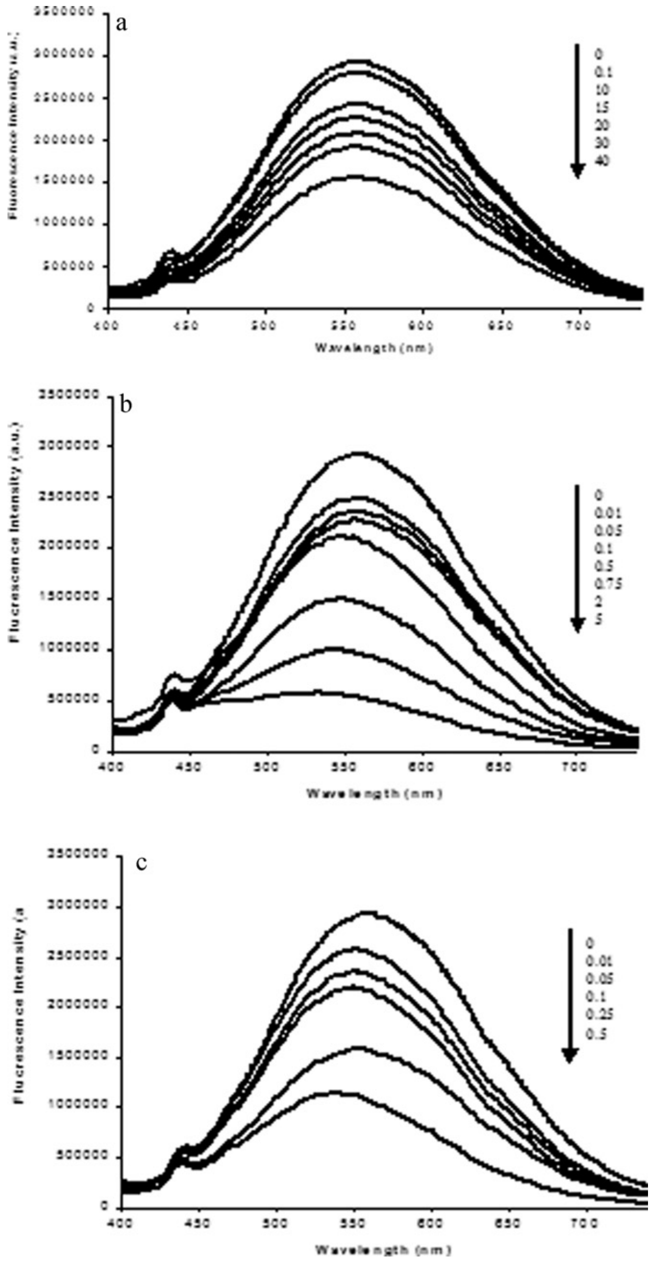

Fig. 2. The effect of nitroaromatic compounds (concentration in mg mL^{-1}) on the emission fluorescence spectrum of the CdSe-PAMAM-G$_4$ nanocomposite: (a.) 4-methoxy-2-nitrophenol (MNP); (b.) 2-amine-5-chloro-1,3-dinitrobenzene (ACNB); and (c.) 3-methoxy-4-nitrobenzoic acid (MNB). CdSe-PAMAM-G$_4$ (500 μL in 5 mL) and [α-CD] = 8.6×10^{-3} M; λ_{ex} = 380 nm; slit = 5.5 nm.

Table 2
ANOVA table obtained from the Plackett–Burman screening design of the concentrations of the three nitrobenzene derivatives, nanocomposite PAMAM + CdSe QDs and α-cyclodextrin (α-CD).

	SS	DF	MS	*F*-ratio	*p*-value	*b*-coefficient	Error
Model	2.82×10^{12}	5	5.64×10^{11}	290	0.0034		
Error	3.89×10^{9}	2	1.94×10^{9}				
Adjusted total	2.82×10^{12}	7	4.03×10^{11}				
Intercept	7.50×10^{13}	1	7.50×10^{13}	3.89×10^{4}	0.000	3.06×10^{6}	1.56×10^{4}
MNP	2.02×10^{10}	1	2.02×10^{10}	10.4	0.084	-1.00×10^{5}	3.12×10^{4}
ACNB	5.62×10^{8}	1	5.62×10^{8}	0.289	0.645	1.68×10^{4}	3.12×10^{4}
MNB	6.31×10^{9}	1	6.31×10^{9}	3.25	0.210	5.62×10^{4}	3.12×10^{4}
Nanocomposite	2.79×10^{12}	1	2.79×10^{12}	1.43×10^{3}	0.001	1.18×10^{6}	3.12×10^{4}
α-CD	5.63×10^{9}	1	5.63×10^{9}	2.89	0.231	5.30×10^{4}	3.12×10^{4}

Table 3
Stern–Volmer parameters for the quenching of the fluorescence of the nanocomposite CdSe-PAMAM by MNP, ACNB and MNB[a]

Nitrobenzene derivative	K_{SV} (M^{-1})	Intercept	R	Points	Concentration (ppm)
MNP	$33(1) \times 10^2$	1.009 ± 0.004	0.991	6	0.1–40
ACNB	$19(2) \times 10^4$	1.169 ± 0.016	0.996	7	0.01–5
MNB	$65(5) \times 10^4$	1.089 ± 0.027	0.988	5	0.01–0.5

[a] Averages and standard deviation (under parenthesis) of three independent experiences.

The analysis of Table 3 shows that the quenching provoked on the nanocomposite fluorescence by the three nitroaromatic compounds follows a simpler Stern–Volmer model. Indeed, besides a correlation coefficient close to one, the intercept is also close to one [46].

The analysis of the magnitude of the calculated Stern–Volmer constants shows that, besides the expected collisional quenching, there is probably the formation of a ground state complex between the nitroaromatic compounds and the CdSe-PAMAM nanocomposite – Fig. 3 shows schematically the resulting structures. Indeed, the comparison of these constants with other corresponding to the quenching of fluorophores by nitrated substances show that the now calculated are several orders of magnitude higher. For example, Goodpaster and McCuffin [51] studied the fluorescence quenching of pyrene and related compounds by nitrated explosives and degradation products and obtained maximum Stern–Volmer constants of nearly four hundreds. Also, they have found that nitroaromatic compounds are more efficient quenchers than their aliphatic counterparts, with higher quenching constants. They have also found that the quenching constants increased with increasing the number of electron withdrawing nitro groups in the benzene ring. In another study using a CdS-DAB dendrimer nanocomposite by nitromethane a $K_{sv} = 25\,M^{-1}$ was observed [39].

The increased affinity of the CdSe-PAMAM nanocomposite towards the studied nitroaromatic compounds may be due to the presence of the dendrimer that undergoes structural modifications as consequence of the presence of the inclusion complex. These modifications on the physico-chemical environmental surrounding the QDs will affect their fluorescence emission properties because it will provoke modifications on the quantum confinement regime.

The effect of another set of nitroaromatic compounds in the sensor fluorescence was studied, namely: trinitrotoluene (TNT); 2,4-dinitrotoluene (2,4-DNT); 2,6-dinitrotoluene (2,6-DNT); and, nitrobenzene (NB). At milimolar concentrations these compounds provoke a relatively small quenching of the sensor fluorescence with the following Stern–Volmer constants: TNT, $K_{SV} = 10(2) \times 10^2\,M^{-1}$; 2,4-DNT, $K_{SV} = 20(3) \times 10\,M^{-1}$; 2,6-DNT, $K_{SV} = 11(4) \times 10\,M^{-1}$; NB, $K_{SV} = 2(1) \times 10^3\,M^{-1}$. The magnitude of the Stern–Volmer constants show that these four nitroaromatic compounds do not interfere at equimolar amounts in the determination of MNB [$K_{SV} = 65(5) \times 10^4\,M^{-1}$] and ACNB [$K_{SV} = 19(2) \times 10^4\,M^{-1}$]. Also, only TNT and NB can interfere when at equimolar amounts with the determination MNP [$K_{SV} = 33(1) \times 10^2\,M^{-1}$] because the Stern–Volmer constant are in the same magnitude.

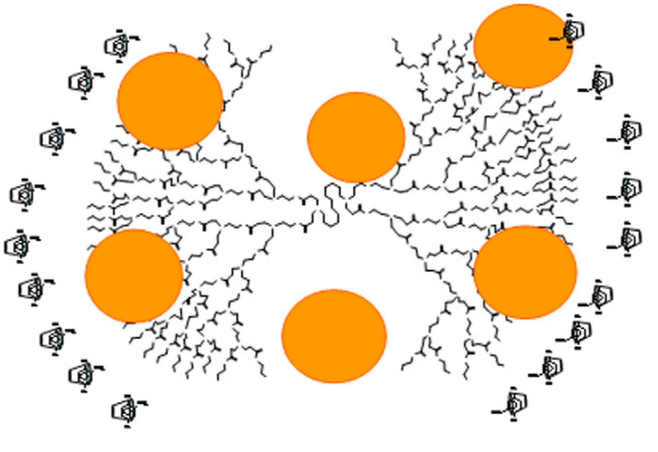

Fig. 3. Schematic representation of the hybrid structure constituted by the CdSe-PAMAM-G_4 nanocomposite, nitroaromatic compounds and α-cyclodextrin.

Tu et al. [52] have observed the quenching of amine-capped ZnS–Mn nanocrystals by TNT and other nitroaromatic compounds, and they have hypothesised that the quenching is due to a strong molecular interaction between the electron-deficient aromatic ring of TNT and the electron-rich amino group of primary amines. The resulting nitroaromatic anions bound to the QDs surface provoking quenching of the fluorescence. Also, they suggest that the stronger the acidity of the nitroaromatic compound is the higher its quenching efficiency. The quenching mechanism proposed by Tu et al. is compatible with the results obtained in the present work, although the chemical system is much more complex as consequence of the presence of the dendrimer and CD. Indeed, the quenching provoked by the strongest acid of the studied nitroaromatic compounds, MNB, is one or two orders of magnitude higher than the others.

The analysis of the emission spectra of the sensor in the presence of the two nitroaromatic compounds that provoke higher quenching (MNB and ACNB) (Fig. 2) shows a slightly blue shift for the higher quencher concentrations. This result may be due to effect of the dendrimer structural modifications in the presence of the inclusion complexes between the nitroaromatic compounds and α-CD.

4. Conclusions

The analysis of nitrated aromatics is an important environmental forensics subject. In this work a new sensor for the detection of some of these substances was described that shows improved sensitivity towards quenching detection.

The sensor described in this work is basically constituted by highly fluorescent nanomaterials (quantum dots – CdSe), that confers the sensor a relatively high analytical signal, and a dendrimer that makes it water soluble and increased reactivity. Moreover, α-CD was used to increase the apparent solubility of the nitroaromatic compounds by inclusion complex formation. As consequence, the presence of these inclusion complexes with the nitroaromatic compounds interacts with the sensor provoking quenching of the fluorescence.

The analytical methodology described for the analysis of nitroaromatic compounds presents a new approach, based on nanomaterials, that is characterized by high quenching of fluorescence sensitivity.

Acknowledgements

The authors would like to thank the Fundação para a Ciência e Tecnologia (Lisboa, Portugal) under the frame of the Ciência 2007 and 2008 programs and FSE-FEDER (Project PTDC/QUI/71001/2006).

References

[1] R. Gatermann, H. Hohnerfuss, G. Rimkus, M. Wolf, S. Franke, Mar. Pollut. Bull. 30 (1995) 221.
[2] J. Yinon, Toxicity and Metabolism of Explosives, CRC Press, Boca Raton, FL, 1999.
[3] N. Talaty, C.C. Mulligan, D.R. Justes, A.U. Jackson, R.J. Noll, R. Graham Cooks, Analyst 133 (2008) 1532.
[4] J. Yinon, D.G. Hwang, J. Chrom. A 268 (1983) 45.
[5] T. Tamiri, S. Zitrin, J. Energetic Mater. 4 (1986) 215.
[6] M. Gaft, L. Nagli, Opt. Mater. 30 (2008) 1739.
[7] M. Ostafin, B. Nogaj, Measurement 40 (2007) 43.
[8] R.I. Jenkinson, J.M. Bradley, G.N. Shilstone, Appl. Magn. Reson. 25 (2004) 439.
[9] J. Fraissard, O. Lapina (Eds.), Explosives Detection using Magnetic and Nuclear Resonance Techniques. NATO Science for Peace and Security Series B: Physics and Biophysics, Springer, Heidelberg, 2009.
[10] C.H. Malden, R.D. Speller, Nuclear Instruments and Methods in Physics Research Section A: Accelerators, Spectrometers, Detectors and Associated Equipment 449 (2000) 408.
[11] A.M. Soldate, R.M. Noyes, Anal. Chem. 19 (1947) 442.
[12] G. Harding, Radiat. Phys. Chem. 71 (2004) 869.
[13] J.P. Hutchinson, C.J. Evenhuis, C. Johns, A.A. Kazarian, M.C. Breadmore, M. Macka, E.F. Hilder, R.M. Guijt, G.W. Dicinoski, P.R. Haddad, Anal. Chem. 79 (2007) 7005.
[14] J.A. Davies, P.A. Hart, G.A. Wood, J. Radioanal. Nucl. Chem. 111 (1987) 71.
[15] I.S. Krull, E.A. Davis, C. Santasania, S. Kraus, A. Basch, Y. Bamberger, Anal. Lett. 14 (1981) 1363.
[16] M. Tam, H.H. Hill, Anal. Chem. 76 (2004) 2741.
[17] N.P. Saravanan, S. Venugopalan, N. Senthilkumar, P. Santhosh, B. Kavita, H.G. Prabu, Talanta 69 (2003) 656.
[18] M. Fischer, J. Georges, Chem. Phys. Lett. 260 (1996) 115.
[19] G. Weber, F.W.J. Teale, Trans. Faraday Soc. 53 (1957) 646.
[20] I. Tredici, D. Merli, F. Zavarise, A. Profumo, J. Electroanal. Chem. 645 (2010) 22.
[21] J.S. Yang, T.M. Swager, J. Am. Chem. Soc. 120 (1998) 11864.
[22] D.T. Mcquade, A.E. Pullen, T.M. Swager, Chem. Rev. 100 (2000) 2537.
[23] H. Sohn, R.M. Calhoun, M.J. Sailor, W.C. Trogler, Angew. Chem. Int. Ed. 40 (2001) 2104.
[24] H. Sohn, M.J. Sailor, D. Magda, W.C. Trogler, J. Am. Chem. Soc. 125 (2003) 3821.
[25] M. Rahman, H.J. Harmon, Spectrochim. Acta Part A 65 (2006) 901.
[26] R. Laureau, in: J.W. Gardner, J. Yinon (Eds.), Electronic Noses and Sensors for the Detection of Explosives, Springer, Heidelberg, 2004, pp. 289–299.
[27] P. Ling (Ed.), Trends in Quantum Dots Research., Nova Science, New York, 2005.
[28] A.Y. Nazzal, L.H. Qu, X.G. Peng, M. Xiao, Nano Lett. 3 (2003) 819.
[29] N. Myung, Y. Bae, A.J. Bard, Nano Lett. 3 (2003) 747.
[30] S.N. Sharma, Z.S. Pillai, P.V. Kamat, J. Phys. Chem. B 107 (2003) 10088.
[31] F. Seker, K. Meeker, T.F. Kuech, A.B. Ellis, Chem. Rev. 100 (2000).
[32] G.C. Lisensky, R.L. Penn, C.J. Murphy, A.B. Ellis, Science 248 (1990) 840.
[33] J.G. Liang, S.S. Zhang, X.P. Ai, X.H. Ji, Z.K. He, Spectrochim. Acta Part A 61 (2005) 2974.
[34] J.M.M. Leitão, H. Gonçalves, C. Mendonça, J.C.G. Esteves da Silva, Anal. Chim. Acta 628 (2008) 143–154.
[35] H. Gonçalves, C. Mendonça, J.C.G. Esteves da Silva, J. Fluoresc. 19 (2009) 141–149.
[36] G.H. Shi, Z.B. Shang, Y. Wang, W.J. Jin, T.C. Zhang, Spectrochim. Acta Part A 70 (2008) 247.
[37] S. Nieto, A. Santana, S.P. Hernandez-Rivera, R.T. Lareau, R.T. Chamberlain, M.E. Castro-Rosario, Proceedings of SPIE – The International Society for Optical Engineering, vol. 5403, 2004, pp. 256–260, Pt. 1, Sensors, and Command, Control Communications, and Intelligence (C31) Technologies for Homeland Security and Homeland Defense III.
[38] E.R. Goldman, I.L. Medintz, J.L. Whitley, A. Hayhurst, A.R. Clapp, H.T. Uyeda, J.R. Deschamps, M.E. Lassman, H. Mattoussi, J. Am. Chem. Soc. 127 (2005) 6744.
[39] B.B. Campos, M. Algarra, J.C.G. Esteves da Silva, J. Fluoresc. 20 (2010) 143.
[40] M.P. Pileni, L. Motte, C. Petit, Chem. Mater. 4 (1992) 338.
[41] Y. Gao, S. Reischmann, J. Huber, T. Hanke, R. Bratschitsch, A. Leitenstorfer, S. Mecking, Colloid Polym. Sci. 286 (2008) 1329.
[42] K.M. Gattas-Asfura, R.M. Leblanc, Chem. Commun. 21 (2003) 2684.
[43] A. Preiss, A. Bauer, H.M. Berstermann, S. Gerling, R. Haas, A. Joos, A. Lehmann, L. Schmalz, K. Steinbach, J. Chromatogr. A 1216 (2009) 4968.
[44] C. Zhang, S. O'Brien, L. Balogh, J. Phys. Chem. B 106 (2002) 10316.
[45] B. Pan, F. Gao, R. He, D. Cui, Y. Zhang, J. Colloid Interface Sci. 297 (2006) 151.
[46] J. Lakowicz, Principles of Fluorescence Spectroscopy, Plenum Press, New York, 1983.
[47] J.C.G. Esteves da Silva, J.R.M. Dias, J.M.C.S. Magalhaes, Anal. Chim. Acta 450 (2001) 175.
[48] P.B.M. Pinheiro, J.C.G. Esteves da Silva, Anal. Bioanal. Chem. 382 (2005) 341.
[49] P.M.S.M. Rodrigues, J.C.G. Esteves da Silva, M.C.G. Antunes, Anal. Chim. Acta 595 (2007) 9.
[50] J.M.M. Leitao, J.C.G. Esteves da Silva, Anal. Chim. Acta 609 (2008) 1.
[51] J.V. Goospaster, V.L. McGuffin, Anal. Chem. 73 (2001) 2004.
[52] R. Tu, B. Liu, Z. Wang, D. Gao, F. Wang, Q. Fang, Z. Zhang, Anal. Chem. 80 (2008) 3458.